

Research



Cite this article: Deng L, Zhang Z. 2018

Assessing the features of extreme smog in China and the differentiated treatment strategy. *Proc. R. Soc. A* **474**: 20170511.
<http://dx.doi.org/10.1098/rspa.2017.0511>

Received: 29 July 2017

Accepted: 19 December 2017

Subject Areas:

applied mathematics, atmospheric science

Keywords:

climate extremes, extreme value analysis, particulate matters, pollution control

Author for correspondence:

Zhengjun Zhang

e-mail: zjz@stat.wisc.edu

Assessing the features of extreme smog in China and the differentiated treatment strategy

Lu Deng¹ and Zhengjun Zhang²

¹School of Statistics and Mathematics, Central University of Finance and Economics, Beijing 100081, People's Republic of China

²Department of Statistics, University of Wisconsin-Madison, Madison, WI 53706-1532, USA

 LD, 0000-0001-5053-5685

Extreme smog can have potentially harmful effects on human health, the economy and daily life. However, the average (mean) values do not provide strategically useful information on the hazard analysis and control of extreme smog. This article investigates China's smog extremes by applying extreme value analysis to hourly PM_{2.5} data from 2014 to 2016 obtained from monitoring stations across China. By fitting a generalized extreme value (GEV) distribution to exceedances over a station-specific extreme smog level at each monitoring location, all study stations are grouped into eight different categories based on the estimated mean and shape parameter values of fitted GEV distributions. The extreme features characterized by the mean of the fitted extreme value distribution, the maximum frequency and the tail index of extreme smog at each location are analysed. These features can provide useful information for central/local government to conduct differentiated treatments in cities within different categories and conduct similar prevention goals and control strategies among those cities belonging to the same category in a range of areas. Furthermore, hazardous hours, breaking probability and the 1-year return level of each station are demonstrated by category, based on which the future control and reduction targets of extreme smog are proposed for the cities of Beijing, Tianjin and Hebei as an example.

1. Introduction

China's smog problem has become very serious and has been receiving attention from government administrators,

ordinary citizens, researchers and international societies. Many known health problems have been documented in the literature. Many health concerns have been raised [1], especially when extreme smog occurs. Fine particulate matter from smoking, the use of solid fuels, etc. contributes significantly to chronic obstructive pulmonary disease, lung cancer, tuberculosis and other related diseases [2,3]. These diseases may lead to millions of deaths from 2003 to 2033 in China [3], which is more than 40 000 premature deaths per year [4]. A long-lasting severe smog in January 2013 prevailed in most main cities in northern China. During this episode, the number of patients with respiratory tract infections and allergic symptoms increased dramatically in hospitals and clinics in Beijing, Tianjin and Shijiazhuang. Studies have indicated that bad air quality in northern China reduces life expectancy by 5.5 years for people living there [5]. The smog also adversely affects China's economy, causes considerable welfare loss [1,6], and has enormous economic and social costs for the world [7,8].

There has been some progress towards solving this problem, e.g. new monitoring technologies have been developed [9,10] and applied in China. Discussions regarding the establishment of collaborative regional policies and compensation systems [11,12], such as the popularization of renewable energy systems and tighter PM_{2.5} controls to prevent future smog crises, have increased [13–15]. Creative methods are also being sought based on lessons learned about smog in the Western world [16–19].

Various studies have been conducted to reveal the masses and chemical compositions of inhalable microorganisms in typical Chinese cities [20–24], as well as the concentrations, formation mechanisms and source apportionments of smog [25–27], especially during significant events [28–34]. Air pollution is related to surface solar radiation and meteorological factors [35], and the impacts of the relative humidity and water-soluble constituents of PM_{2.5} on visibility impairment have been modelled [36]. In addition to physical and chemical explanations, assessments of China's virtual air pollution transport through economic and trade activities have also been studied using a consumption-based emission inventory [37]. Moreover, because PM_{2.5} concentrations are significantly influenced by meteorological conditions [30,33], statistical approaches have been proposed to adjust the PM_{2.5} concentrations of Beijing using data from 2010 to 2015 [38].

Understanding the features of smog extremes across China is vital for the government to carry out differentiated treatments in cities with different extreme features and jointly implement a control strategy within those bearing similar characteristics. One common point of view shared by the above research is that China's smog is extreme in duration, frequency and severity [24,29]. The average number of smog days in China in 2013 reached the highest point in 52 years in 13 provinces, about one-third of the national territorial area. In 2015, 11 rounds of persistent smog covering a broad range of areas occurred, especially in the last two months of the year. Heavy air pollution continued for 5 days at the end of November 2015, with the PM_{2.5} concentrations of most stations in Beijing exceeding $400 \mu\text{g m}^{-3}$ and those stations in south Beijing reaching concentrations of more than $900 \mu\text{g m}^{-3}$. Various studies based on the averaged data or the annually averaged satellite-derived estimates have been reported in the literature [39–41]. Owing to the significant threat and harm to the economy, human health and welfare that China's extreme smog causes, it is vital to model and study its extreme characteristics. After all, severe smog levels are more dangerous than ordinary levels. To the best of our knowledge, the features of nationwide extreme smog have not been studied in any depth, and neither have systematic statistical analyses of the properties of extreme smog in China been carried out.

The main objective of this research was to conduct extreme value analysis of China's smog extremes using PM_{2.5} data between 2014 and 2016 from air quality monitoring stations across China. We found that the characteristics of extremes varied not only with time within any single station but also across different locations. By fitting the generalized extreme value (GEV) distribution, monitoring stations were designated to eight categories according to the fitted mean values and shape parameter estimates of the GEV distributions. The fitted mean represents the average level of extreme smog, and it is classified by referring to the PM_{2.5} breakpoints from the US (EPA) standard [42]. The sign of the shape parameter determines the maximum frequency

and upper bound of the extreme smog that may occur. The features of the eight categories are then demonstrated to aid the government in performing targeted treatment measures. Moreover, the ultimate control target of the cities of Beijing, Tianjin and Hebei proposed by this study to reduce the number of severe pollution days, frequency and maximum level of PM_{2.5} could yield a significant air pollution regional cooperation simulation benchmark and provide insights into the possible future strategy of pollution treatment. Given the needs of the Beijing–Tianjin–Hebei integration strategy and the air pollution control target for the 2022 Winter Olympics, the obtained results could be particularly useful. As such, they can further help to improve the national air quality forecasting system for the major regions and cities and to benefit public health and the economy. The analyses conducted in this study are better than other analyses applying a conventional mean analysis approach whose focus was on the average levels of smog, i.e. not on the extreme levels of smog which are mostly concerned by a pre-warning system.

2. Data and methods

(a) Data

The data we use are the hourly PM_{2.5} data obtained from air quality monitoring stations located in China during 2014–2016. The data source is the China National Environmental Monitoring Centre. There were 945 recording monitoring stations in 2014, most of which were built downtown of the major cities to sample the air quality where the majority of people live. The locations of each province are shown in figure 1. Among these stations, Guangdong province (25 in figure 1*a*) in south China and two provinces in east China (Shandong and Jiangsu, 4 and 5 in figure 1*a*) contain the most stations (102, 100 and 97 in 2014, respectively). The provinces located in southeast China had more stations than those inland, especially west China. It is worth noting that the number of stations also reflects the regional economic development. The station coverage rate increased dramatically in 2015 (up to 1496 stations) and 2016 (total 1497 stations). As a result, most of the provinces are evenly equipped with monitoring stations.

Note that, at the time of data recording, some stations were still under testing or had data transition problems, hardware failures, and probably delayed updates. As a result, some data were missing or taken as zero. In our analysis, those stations with 50% or more zeros within the data were removed from our analysis list. As such, approximately 936 stations out of 945 qualified for analysis in 2014, and 1480 stations qualified for analysis in 2015 and 2016.

(b) Threshold and extreme values

To determine the extreme characteristics of the data, we first note that a 90% or higher quantile as a threshold level is commonly used in the literature regarding extreme value distribution fittings. Also, extreme values at a given station are station specific, i.e. it is not appropriate to compare them with extreme values from a different station. In this study, we consider a typical threshold level, i.e. the 90% quantile, so that the extreme values from each station are those exceeding the chosen threshold (the choice of threshold will be discussed further in §2*c*). A station-specific threshold means that the observed extreme values of smog are equal to or higher than the threshold during one-tenth of the year. It is easy to see that the higher the threshold, the more severe the extreme smog is at the station. From the pollution point of view, one may choose a common high level of PM_{2.5}, e.g. a level related to health hazard exposure, in distribution fittings. However, such a choice will lead to some potential problems. Taking a threshold of $250.5 \mu\text{g m}^{-3}$ as an example, the number of extreme values for stations in Tibet will be much smaller than that for stations in Hebei. As a result, we would not be able to determine the extreme characteristics of smog in Tibet in terms of an extreme value distribution fitting.

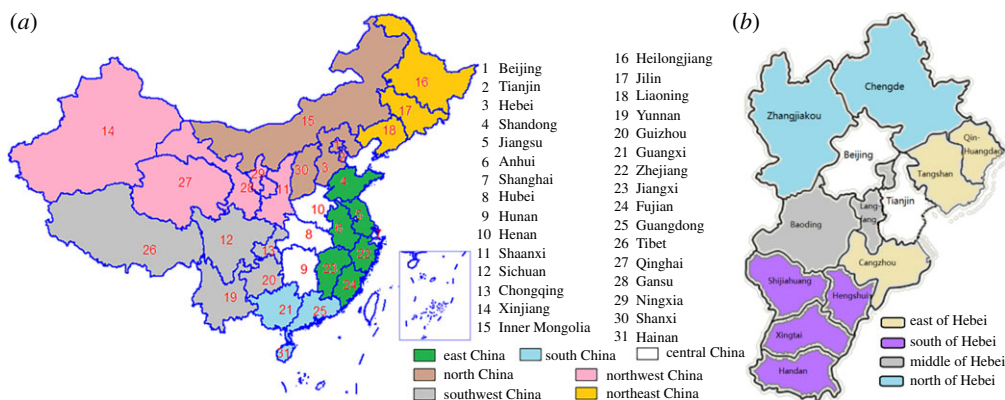


Figure 1. (a) Provinces in China and (b) cities in the Beijing–Tianjin–Hebei region.

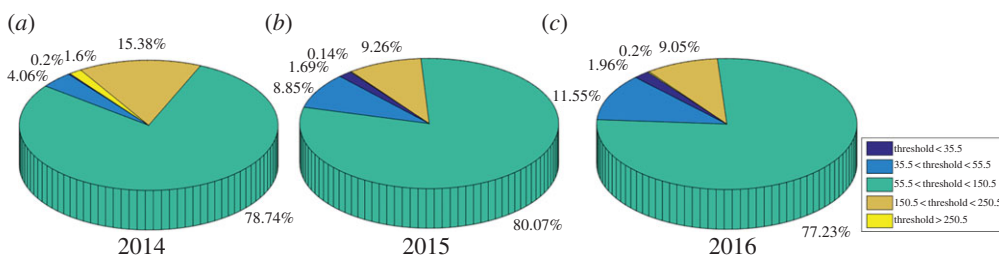


Figure 2. (a–c) Pie charts of the relative percentages of thresholds ($\mu\text{g m}^{-3}$) from 2014 to 2016.

As extreme smog does not uniformly spread over a region and monitoring stations, the thresholds vary from one station to another. Figure 2 shows the percentages of station-wide thresholds that fall into different intervals defined by the US (EPA) standard. There are five intervals of PM_{2.5} level according to the US (EPA) standard, which have different implications for human health. The breakpoints of each interval are as follows: (i) $35 \mu\text{g m}^{-3}$ is the highest PM_{2.5} level for acceptable air quality (good and moderate category); (ii) the range from 35 to $55.4 \mu\text{g m}^{-3}$ is said to be unhealthy for sensitive groups; (iii) the range from 55.5 to $150.4 \mu\text{g m}^{-3}$ is unhealthy; (iv) above $150.4 \mu\text{g m}^{-3}$ is widely viewed as very unhealthy; and (v) levels above $250.5 \mu\text{g m}^{-3}$ is considered to be hazardous. It can be seen that the air quality improved from 2014 to 2016 from the view of extreme smog. Less than 1% of the stations in 2014 had an acceptable air quality (threshold $< 35.5 \mu\text{g m}^{-3}$) during at least nine-tenths of the year. This percentage increased to 2% in 2015 and 2016. The percentage of thresholds from 35.5 to $55.5 \mu\text{g m}^{-3}$ increased from 4.06% in 2014 to 8.85% in 2015, and then to 11.55% in 2016. Most stations are defined as having extreme smog with thresholds from $55.5 \mu\text{g m}^{-3}$ to $150.4 \mu\text{g m}^{-3}$. Approximately 17% of stations have extreme smog of a very unhealthy or even hazardous level (greater than $150.5 \mu\text{g m}^{-3}$) during one-tenth of the year. This percentage dropped to less than 10% after 2015.

From figure 2, one can see two extreme scenarios with relatively small proportions, i.e. the case of the 90% quantile threshold levels being less than $35.5 \mu\text{g m}^{-3}$ and the case of the threshold levels being greater than $250.5 \mu\text{g m}^{-3}$. All station thresholds vary from time to time and also from location to location. It is clear that high thresholds are good descriptive statistics that tell how severe the smog is in a particular region where a monitoring station is located. However, they do not deliver much information for inference, worst case scenario prevention, a joint control strategy or a reduction target. It is not possible to say that the air quality in a region with a greater than 90% quantile threshold level is much worse than that in another region with a lower threshold level.

Another fundamental problem is what the worst case smog scenario is in a particular region. To address these issues, we have to take a careful look at the exceedance values over the threshold and to extract the extreme features from them. To achieve this goal, we applied extreme value analysis to the smog extremes.

(c) Method

We start with a brief review of extreme value analysis methods. There are three common approaches in the extreme value analysis literature. They are the block maxima approach, the peak over threshold approach, which fits a generalized Pareto distribution to exceedances over a threshold, and the point process approach, which also involves a threshold value in a GEV distribution fitting.

There is no consensus on which method should be used. The choice depends on whether or not the data satisfy the assumption of the chosen approach. For example, the fitting of the GEV distribution usually assumes that the data are i.i.d. However, the hourly data we are dealing with can be potentially time-dependent and non-stationary. Therefore, the point process approach, which is robust under these circumstances, was preferred in this applied project. The advantage of applying the point process to the distribution fitting is discussed in Coles [43] and Smith [44]. Besides, there are also some seasonal variations in PM_{2.5} values. For example, winter in northern China probably has higher PM_{2.5} values due to the burning of coal. The point process approach can naturally solve this problem to some extent. Under this framework, the extreme values are those exceeding a chosen threshold, and they often form clusters in wintertime and springtime (to be more specific, the first and the fourth seasons) instead of other seasons. The GEV fitting of these extremes can well recover the extreme characteristics of the whole year. As such, the few data points in the second and third seasons need not be fitted separately.

The classical point process approach usually requires the length of the extreme values to be 5–10% of the total sample size. To guarantee a sufficient data size of extreme values, a 90% quantile was chosen to be the threshold in this paper so that the number of extreme values above the threshold was 10% of the total sample. Taking an average of 365 days per year as an example, we have 8760 hourly data points in total. The observed number of occurrences of extreme values for each station was 876. This number can also lead to smaller variances in the estimators of the GEV distribution mentioned below (taking the shape parameter estimators of each station as an example, most of which have a standard deviation smaller than 0.05).

The GEV distribution has a cumulative distribution function as follows:

$$F(x) = \begin{cases} \exp \left\{ - \left(1 + \xi \frac{x - \mu}{\sigma} \right)^{-1/\xi} \right\} & 1 + \xi(x - \mu)/\sigma > 0, \xi \neq 0 \\ e^{-e^{-\frac{x - \mu}{\sigma}}} & \xi = 0. \end{cases} \quad (2.1)$$

There are three important parameters in the above equation, where μ is a location parameter and $\sigma > 0$ is a scale parameter that is similar to the standard deviation of a random variable. ξ is a shape parameter that leads to different types of distributions and shapes (skewness and tail length) of the density functions. To be specific, when $\xi < 0$, $F(x)$ is the type III or Weibull distribution, and its probability density is zero if $x > -\sigma/\xi + \mu$, i.e. the density (left-skewed) has an upper bound $-\sigma/\xi + \mu$ and a short tail. When $\xi > 0$, $F(x)$ is the type II or Fréchet distribution, and its probability density (right-skewed) is zero if $x < -\sigma/\xi + \mu$, i.e. the density has a lower bound $-\sigma/\xi + \mu$ and a long right tail. The limit $\xi \rightarrow 0$ corresponds to the type I or Gumbel distribution; there is no upper or lower bound for the density (right-skewed) [43]. One can see that the shape parameter ξ determines the skewness and tail length (bound), i.e. the shape of the density.

The expectation function is

$$E(x) = \mu + \sigma(\Gamma(1 - \xi) - 1)/\xi, \quad \xi \neq 0, \quad \xi < 1, \quad (2.2)$$

where $\Gamma(\cdot)$ is the gamma function. In the case of $\xi = 0$, it becomes

$$E(x) = \mu + \sigma \gamma, \quad (2.3)$$

where γ is Euler's constant.

The expectation function represents the average level of extreme smog and could be used to classify stations into groups with different air quality. However, under similar expectations, the severity of extreme smog between two stations also depends on their corresponding shape parameters, which lead to different skewness and tail lengths of the density functions. For stations with a right-skewed density, the mode is lower than the mean; while for those with a left-skewed density, the mode is higher than the mean. As a result, a station with a left-skewed density will have more values clustered at high levels than a station with a right-skewed density, i.e. the station with a left-skewed density will suffer more intensive extreme smog occurrences. It is also interesting to note that, although the left-skewed density leads to more intensive extreme smog, it has an upper bound, i.e. the probability that the extreme smog exceeds the bound is zero. On the other hand, when a right-skewed density has a very long tail, the extreme smog could be very severe, but with a very low probability. For the latter case, the occasional very high PM_{2.5} level could occur. In other words, the two types of stations according to different signs of their fitted ξ values have distinct extreme smog features that should be handled differently.

While some features of extreme smog can be extracted using the expectation function and shape parameter, there are also certain scenarios of extreme smog that very much concern the general public, taking the duration and frequency of certain PM_{2.5} levels as an example. To tackle these problems, we further compute the following three quantities, in which the risk of extreme smog at certain individual high levels or the maximum level of extreme smog under certain circumstances can be derived. In this way, the worst case scenario can be investigated and then prevented, and corresponding reduction targets can also be made.

Different from the studies of climate extremes in precipitation, temperature and snowfall, which are mostly concerned with their annual maxima, the studies of extreme smog are more concerned with levels during a single year, or even during a single day. The reason for this is that the PM_{2.5} concentration at one station may grow to very high levels during one single day due to adverse meteorological factors and the accumulation of contaminants, especially in the winter. As a result, the hourly data for each year are used separately to fit the GEV distribution in this paper to capture the rapid variations in extreme smog, and then the following quantities are used to demonstrate the occurrences of extreme smog within 1 year.

The mean times of exceedance over a specified high level x within 1 year is given by

$$N_{\text{mean}} = m(1 - F(x)) = m \left\{ 1 - \exp \left[- \left(1 + \xi \frac{x - \mu}{\sigma} \right)_+^{-1/\xi} \right] \right\}, \quad \xi \neq 0, \quad (2.4)$$

where $m = 876$. Note that 876 h of data per year are used to fit the GEV distribution in this paper. This quantity can be used to evaluate the frequency of certain high-level extreme smog events.

The probability of extreme smog exceeding a specified high level x at least once within 1 year, which describes the risk of extreme smog at certain individual high levels, is given by

$$p_{\text{level}} = 1 - (F(x))^m = 1 - \left\{ \exp \left[- \left(1 + \xi \frac{x - \mu}{\sigma} \right)_+^{-1/\xi} \right] \right\}^m, \quad \xi \neq 0. \quad (2.5)$$

The 1-year return value is

$$x_{\text{return}} = \begin{cases} \mu - \frac{\sigma}{\xi} \left[1 - \left\{ -\log \left(1 - \frac{1}{m} \right) \right\}^{-\xi} \right] & \xi \neq 0 \\ \mu - \sigma \cdot \log \left(-\log \left(1 - \frac{1}{m} \right) \right) & \xi = 0. \end{cases} \quad (2.6)$$

This indicates the maximum value of extreme smog occurring on average once within a year. The 1-year return value is another way to describe the risk of extreme smog at a certain frequency. The higher the return level, the more severe the extreme smog will be on average.

The parameters in the GEV distribution are estimated using the maximum-likelihood method based on the point process approach mentioned above. All the estimators are asymptotically normal. The significance test can be used for each single station successively. However, this may result in a greatly increased false positive rate. Taking the shape parameter ξ as an example, the significance test is used to test the null hypothesis $\xi = 0$. Rejecting the null hypothesis may indicate the intensity of the extreme smog being severe (in the case of $\xi < 0$, as mentioned above). However, due to the large number of stations, the above testing procedure may result in a significant increase in the total number of stations that falsely reject the null hypothesis, which may result in a large number of stations reporting very severe extreme smog.

To solve this problem, we use a practical and powerful approach to multiple testing [45,46] by controlling the false discovery rate at a level of 0.05. As a result, the intensity of extreme smog at each station can be determined more accurately so that the exact features of extreme smog can be derived. For the location and scale parameters, multiple testing can also help to determine whether their real values are zero, which affects the valid computation of the estimated mean value of extreme smog.

3. Features of the extreme smog and stations classification

It is conventional to rank the air quality of different areas using averaged PM_{2.5} data (24 h or annual averages) [39–41]. For example, to tackle the PM_{2.5} problem, Van Donkelaar *et al.* [40,41] generated global satellite-derived PM_{2.5} concentration estimates, which enable the evaluation of smog long before some areas, especially in developing countries, can build ground-level monitors. Quantities of studies have been done using their PM_{2.5} map of annually averaged data from the period 2001–2006 [40] and their improved data from the period 2001–2010 [39,41]. This paper intends to investigate the smog extremes by categorizing the stations rather than simply ranking them by the average of extreme PM_{2.5} values. For a simple scenario of the 24-hour average PM_{2.5} levels in two stations being larger than $250.5 \mu\text{g m}^{-3}$, it does not mean much to rank them only because they are both hazardous to people's health. This paper tries to derive the features of extreme smog at each station by fitting the GEV distribution, according to which the stations are then categorized and result in different measures to facilitate specific treatment activities.

First, we use the estimated mean (computed by the fitted GEV parameters using equations (2.2) and (2.3)) of the GEV distribution to classify the stations. (The sample mean of the extreme value can also be used to classify stations, which is an unbiased estimator of the expectation, while the estimated mean computed by the fitted GEV parameters is asymptotically unbiased and consistent. Both of the estimators were computed for comparison when classifying the stations, and very similar results were obtained. For simplicity, only the results of the estimated mean are given in this paper.) The estimated mean represents the annual average level of extreme smog at each station. Stations are then classified based on the intervals their estimated means fall into. The intervals are determined according to the PM_{2.5} breakpoints from the US (EPA) standard mentioned in §2b, which relate to different levels of air quality. Therefore, the classified groups of stations correspond to areas with different levels of air quality and health concerns driven by the average level of extreme smog. Since only a few stations have an estimated mean below $35 \mu\text{g m}^{-3}$ or from 35 to $55.4 \mu\text{g m}^{-3}$, they form group I (relatively speaking, the best group). Stations with an estimated mean from 55.5 to $150.4 \mu\text{g m}^{-3}$, those from 150.4 to $250.5 \mu\text{g m}^{-3}$ and those above $250.5 \mu\text{g m}^{-3}$ form group II, group III and group IV (the worst group), respectively. More groups are also possible, but they may not be necessary when management by the government is taken into account in practice.

The station's spatial distribution of these four groups is shown in figure 3. The results of 2014–2016 showed that the stations in group IV were mainly located in a large connected area

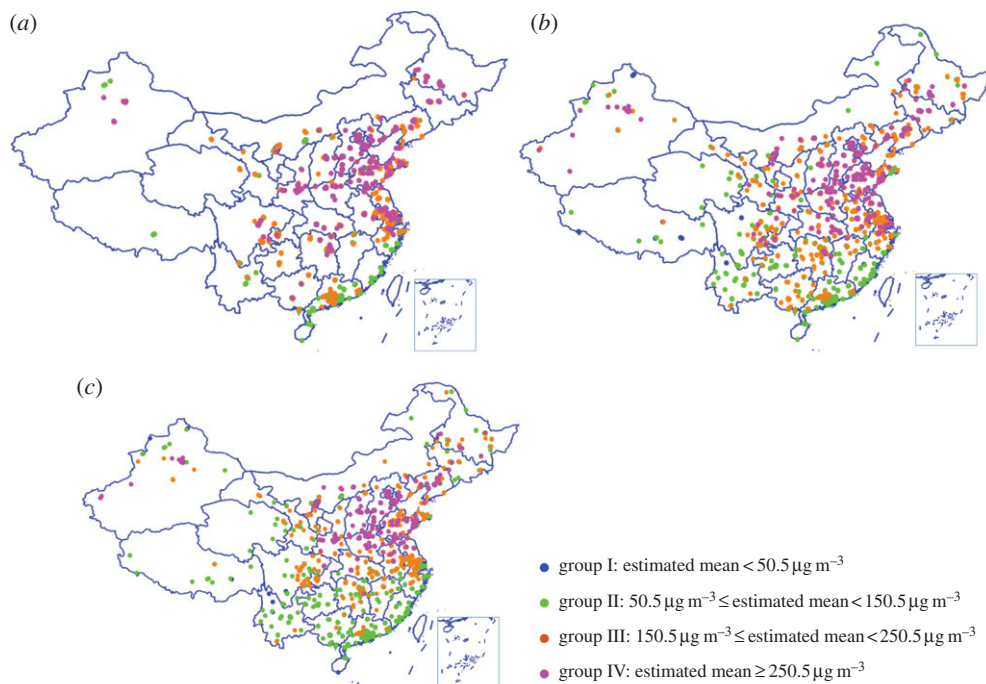


Figure 3. The annual spatial distribution of the average level of extreme smog. The monitoring stations are represented by colourful dots, which give each station's longitude and latitude to show its geographical position; (a–c) years 2014–2016, respectively.

including north China, northeast China, central China, two provinces (Shaanxi and Xinjiang; their geographical locations are numbered 11 and 14 in figure 1a, respectively) in northwest China, several provinces (Shandong, Jiangsu, Anhui, etc.) in east China, and even a few areas (e.g. Sichuan, numbered 12 in figure 1a) in southeast China. This connected area was associated with 16 provinces in 2014. Note that the number of stations located to the south of the Huaihe River decreased dramatically in 2016. For stations in group IV, they experienced extreme smog with an annual average level greater than or equal to $250.5 \mu\text{g m}^{-3}$ during 10% of the whole year. This greatly endangered people's health. The percentage of stations in group IV was 26.8% in 2015 and this figure dropped to 22% in 2016. The extreme smog in Yunnan and Guizhou (numbered 19 and 20 in figure 1a, respectively) within southwest China and the regions in south China was relatively lighter than the extreme smog in other regions, but the annual average was still between 55.5 and $150.4 \mu\text{g m}^{-3}$. The percentage of stations in group II was 30% in 2015 and this increased to 43% in 2016. The stations in group I appeared sparsely in Tibet (numbered 26 in figure 1a), etc. with the annual average level of extreme smog being lower than $55.5 \mu\text{g m}^{-3}$. This caused, relatively speaking, the least harm to human health, but the number of group I stations amounted to only 1% in 2015 and 2016. The remaining stations belonged to group III, with an average extreme PM_{2.5} level of 150.4 – $250.5 \mu\text{g m}^{-3}$. The percentage of group III stations was 42% in 2015, which dropped to 34% in 2016. In all, the extreme smog showed some improvement in 2016 in that the percentage of group III and group IV stations decreased in 2016 while the percentage of group II stations increased.

Existing research based on the estimated PM_{2.5} data before 2011 also gave some results on the distribution of severe smog. It was demonstrated that high concentrations of PM_{2.5} were mostly found in regions of East Asia with high population densities, including the Beijing–Tianjin–Hebei region (see figure 1b) in north China, east China (including the Shandong, Anhui and Jiangsu provinces) and Henan province [39–41]. It also showed some basin effects, such as in the Sichuan Basin and Xinjiang Basin [47]. The above results were consistent with our findings on group IV to

some extent, showing that the severe smog problem in these areas was sustained all the time and hardly improved in recent years.

Annual means of PM_{2.5} values from 2014 to 2016 at all monitoring stations across China were also computed in this paper for comparison. It is shown that the above results regarding the extreme smog differ from those regarding the annual means. We found that although stations in northeast China and to the north of Hebei (Zhangjiakou and Chengde, the locations of cities in Hebei are drawn in [figure 1b](#)), etc. had relatively lower annual means than others (best 30% of all stations), their average levels of extreme smog were relatively higher (the worst third among all stations). Such a phenomenon was due to the fact that there were extreme PM_{2.5} values during some period although their annual air qualities were relatively good on average. On the contrary, stations in some areas were often ‘misunderstood/regarded as having extreme smog’ because their annual means of PM_{2.5} values were relatively higher (the worst third among all stations). In fact, the volatility of PM_{2.5} levels for these stations was not very large while the average level of extreme smog was not very high either (best 30–50%). Taking an example from stations in two provinces (Sichuan and Chongqing, numbered as 12 and 13 in [figure 1a](#)) in southwest China and two neighbouring provinces (Hubei and Hunan, numbered as 8 and 9 in [figure 1a](#)) in central China, different conclusions can be drawn if the average levels of extreme smog rather than the overall means of smog are used. This paper focuses on extreme smog due to the great harm that extreme smog can do to human health, the economy and normal life.

Under similar average levels of extreme smog, the features of extreme smog also depend on the shape parameter ξ , which leads to different skewness and tail length of the density. As mentioned above, for stations with a left-skewed density, the PM_{2.5} level at the maximum frequency is relatively high, i.e. higher PM_{2.5} levels happen for longer, thus the air quality is more often poor. For stations with a right-skewed density of extreme smog, the PM_{2.5} level at the maximum frequency is relatively low, which means that relatively good air quality happens more frequently. However, there exist very high PM_{2.5} levels occasionally for these stations due to the long tail of the density, which greatly enhances the average levels of extreme smog. Considering all of these combinations, we further divide each of the four groups (I–IV) of stations into two parts, which are represented by the categories I-R, I-L, II-R, II-L, III-R, III-L, IV-R, IV-L, respectively (R represents stations with a right-skewed density and L represents those with a left-skewed density). The spatial distribution of the eight categories of stations across China is illustrated in [figure 4](#). The eight categories of stations have distinguishing features for extreme smog.

For the whole country (the spatial distribution of eight categories is referred to [figure 4](#), and the percentage is shown in [figure 5](#)), the percentages of I-R and II-R increased considerably in 2016 while the percentages of III-L and IV-L decreased, which showed a general improvement in extreme smog throughout the country. In addition, the number of right-skewed stations was larger than the number of left-skewed stations within the same group. This indicates that, for most stations, the occasional bout of very severe smog augments the average level of extreme smog greatly.

Specifically, stations in northeast China were mainly in categories IV-R and III-R, indicating that there occasionally exists very severe extreme smog in this area. However, for most of the time, this region experiences relatively lower PM_{2.5} levels than the IV-L and III-L stations. These features can also explain why, for stations in northeast China, their average levels of extreme smog rank better than the annual means. The occasional very high PM_{2.5} levels could have specific causes during a particular time, such as the beginning of the colder seasons when coal burning increases [48]. Acknowledging these features will benefit the corresponding policy-making to suit the specific cause.

It is worth mentioning that in Beijing–Tianjin–Hebei, where the most important closely connected group (both geographically and economically) in north China is located, the percentage of stations in group IV amounted to 90% in 2014 and 75% in 2016, indicating that extreme smog at most stations in this area reached a very high level. Taking the year 2014 as an example, except for the north of Hebei (Zhangjiakou and Chengde), all stations belonged to group IV (90% as

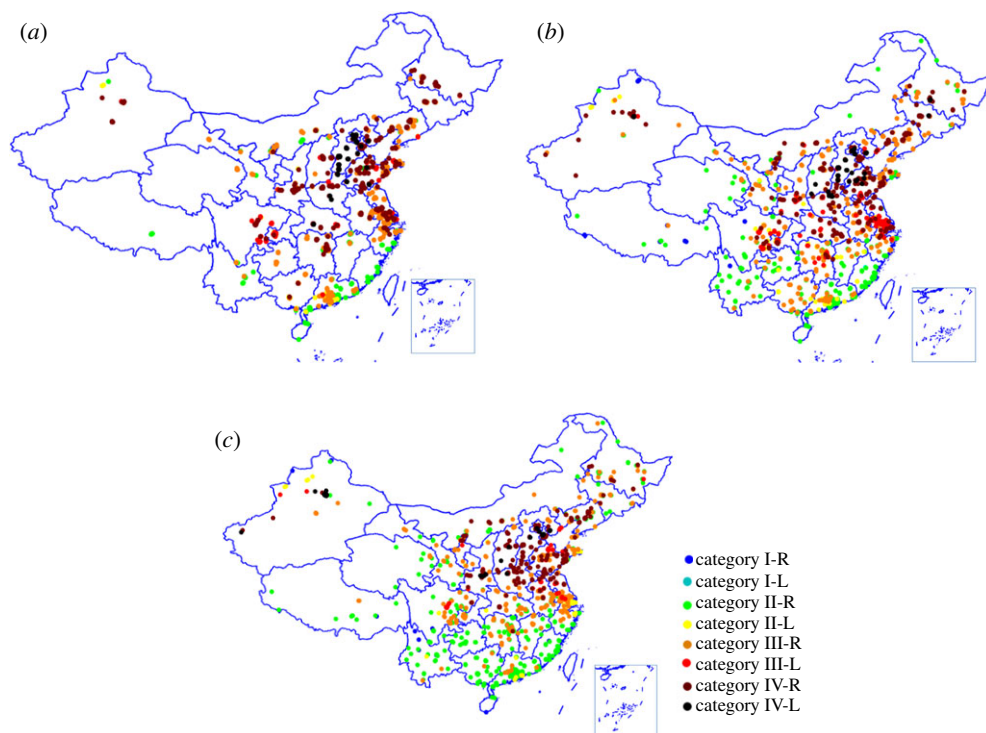


Figure 4. The spatial distribution of the eight categories of stations across China; (a–c) years 2014–2016, respectively.

mentioned above). However, half of these fell into category IV-R (including 13 out of 14 stations in Tianjin), while the remaining ones belonged to category IV-L (including seven out of 12 stations in Beijing, etc.).

The features of extreme smog for these two kinds of stations are different. The PM_{2.5} level at the maximum frequency (x_{mode} , which is the most common recurring level of extreme smog) at IV-L stations was much higher than that at IV-R stations, showing more intensive extreme smog. For example, x_{mode} was about 200–230 $\mu\text{g m}^{-3}$ for stations in Tianjin and was even close to 300 $\mu\text{g m}^{-3}$ for those IV-L stations in the middle and south of Hebei. The possible reasons for this are that for IV-L stations the amounts of contaminants are sustained at high levels in these areas because of adverse meteorological conditions, a lot of local motor vehicles or the long-term inputs of extraneous pollutants from adjacent areas, etc. [33]. For these situations it is more effective to focus on all sources of pollutants and implement normalized emission reductions and preventions.

There were also some notable changes during 2014–2016. The percentage of IV-L stations in Beijing–Tianjin–Hebei was 45.6% in 2014, which constituted 81% of all IV-L stations in China. These two percentages decreased dramatically to 12.5% and 27%, respectively, in 2016, showing a great improvement in air quality. For IV-R stations in Beijing–Tianjin–Hebei, the two percentages were 46.8% and 12.8% in 2014, which increased, respectively, to 62.5% and 17.3% in 2016. Specifically, most stations in the provincial capital (Shijiazhuang) changed to category IV-R in 2016 from category IV-L; in these cases, their level of extreme smog at the maximum frequency may decrease. Similar changes also happened in Beijing, and other cities in the middle (Baoding, Langfang) and southern Hebei (Handan, Hengshui and Xingtai). The locations of these cities are shown in figure 1*b*.

Furthermore, cities across China are classified into these eight categories according to the category that most stations within each city fall into. As PM_{2.5} monitoring stations mostly are located in the downtown areas of cities, categorizing cities according to the features of extreme

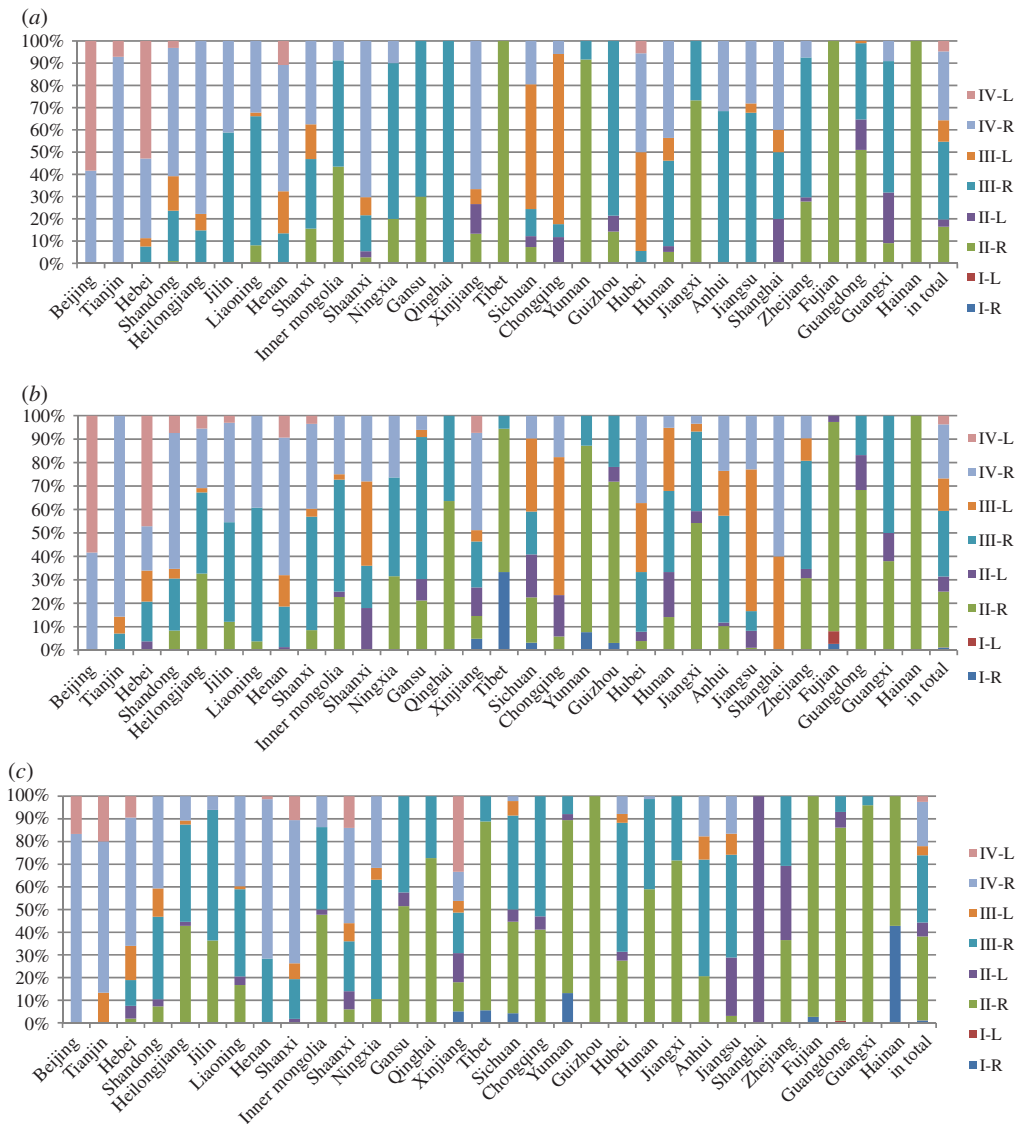


Figure 5. The percentage of eight categories of stations in each province. (a–c) Bar graph for the years 2014–2016, respectively. The last bar in each graph shows the percentages of the eight categories for the whole country.

smog at each station can better demonstrate the overall features of a larger area. Owing to the complexity of the number and distribution of stations in each city, it is hard to find a generally applicable algorithm to classify cities without extensive computations and validation, which is outside the scope of this paper. However, following the general rule of meteorology, the PM_{2.5} monitoring stations are set up as evenly as possible in cities. Therefore, the simple majority rule is used as it is the most practicable.

It is interesting to note that the IV-L cities in our study closely match the cities with the worst air quality announced previously [49,50]. For example, the eight IV-L cities in 2015 are Beijing; Shijiazhuang, Tangshan, Baoding, Langfang, Hengshui and Xingtai in Hebei province (as shown in figure 1*b*), all of which are located in the area of Beijing–Tianjin–Hebei; and Zhengzhou in Henan province. All cities but Beijing were also included in the top 10 worst air quality cities according to the 2015 annual average air quality index (AQI) figures published by the Ministry of Environmental Protection of China [49]. This match between our results and the official report

also shows that the main air pollution in China is usually PM_{2.5}, which contributes considerably to the high AQI. However, in spite of this, Beijing was on our list, but it was not on the official list, indicating that the rank of Beijing in terms of extreme smog was worse than its relative rank in terms of the annual means, implying that low annual means do not guarantee that extreme values do not exist.

4. The risk and maximum level of extreme smog: hazardous hours, breaking probability and 1-year return level

In the previous section, the features of extreme smog driven by the average level of extreme smog and the shape of its density function were demonstrated. In this section, the following three quantities were further computed to analyse certain worst case scenarios of extreme smog that concern the general public. The confidence intervals of the three quantities computed via the multivariate delta method are available to readers on request.

First, the average number of times that the PM_{2.5} value exceeds $250 \mu\text{g m}^{-3}$ within 1 year (N_{mean}) was considered (it is computed using equation (2.4) with $x = 250$). This indicates the times (i.e. hours in this paper) that the air quality appears hazardous or even worse (therefore, it is called ‘hazardous hours’ for short), which may lead to great harm to human health. Determining the number of hours that hazardous air quality lasts for can be of benefit when devising strategies aimed at reducing the duration of severe pollution.

Figure 6*a–c* shows box plots of N_{mean} from 2014 to 2016. The figure shows that the hazardous hours within 1 year for stations in group I is zero, and for those in group II it was very close to zero, meaning that the air quality in these two groups was better than the hazardous level. There were some hazardous hours for stations in categories III-R, III-L, IV-R, IV-L, which increased successively, i.e. the hazardous smog became worse for these four categories. The hazardous hours for III-R and III-L approximate each other to some extent, which was about 100 h on average. For stations in category IV-L, the average duration of N_{mean} was about 650 h in 2014, about 600 h in 2015 and below 600 h in 2016. Although this showed a declining trend, it still covered 6.8% of the whole year, i.e. 1 day out of 14.6 days had a hazardous air quality. While the number of hazardous hours for stations in category IV-R were one-half to two-thirds less, this still amounted to one hazardous day every 29.2 to 43.8 days.

The probability that the PM_{2.5} value exceeds $500 \mu\text{g m}^{-3}$ within 1 year (p_{level}) was also determined (this is computed using equation (2.5) with $x = 500$). This is called the ‘breaking probability’ in this paper. The word ‘breaking’ is used here because $500 \mu\text{g m}^{-3}$ is the maximum value that is given in the US standard. Whether the PM_{2.5} value exceeds $500 \mu\text{g m}^{-3}$ is of great concern to the general public in China. If this maximum level is exceeded, it causes significant distress to residents. Stations in most categories had certain breaking probabilities, a decrease in which can also be considered as one of the valuation approaches to smog reduction. Figure 6*d–f* shows box plots of the p_{level} . It was shown that, for stations in categories I-L, II-L and III-L, most p_{level} values were zero or close to zero, meaning that the PM_{2.5} values in these areas were not likely to exceed $500 \mu\text{g m}^{-3}$. For stations in categories I-R, II-R and III-R, however, the density of extreme smog had a long tail, which means that the p_{level} will be greater than zero. However, for these stations, the very high PM_{2.5} levels only occurred occasionally. In other words, the breaking probabilities were very small but they did exist. As far as the medians in figure 6*b–f* were concerned, they were around 0.2 for stations in categories I-R, II-R and III-R (except for category III-R in 2014). It was demonstrated from p_{level} that the features of extreme smog at left-skewed stations were very different from those at the right-skewed ones, requiring different treatment measures.

The breaking probabilities equalled 1 for most stations in category IV-L with certain times of breaking. Although the extreme smog in these stations had an upper bound, it is obviously higher than $500 \mu\text{g m}^{-3}$. The breaking probabilities for some stations in category IV-R were also rather high and even approached 1. In some cases, this shows certain breaking times. Owing to the great

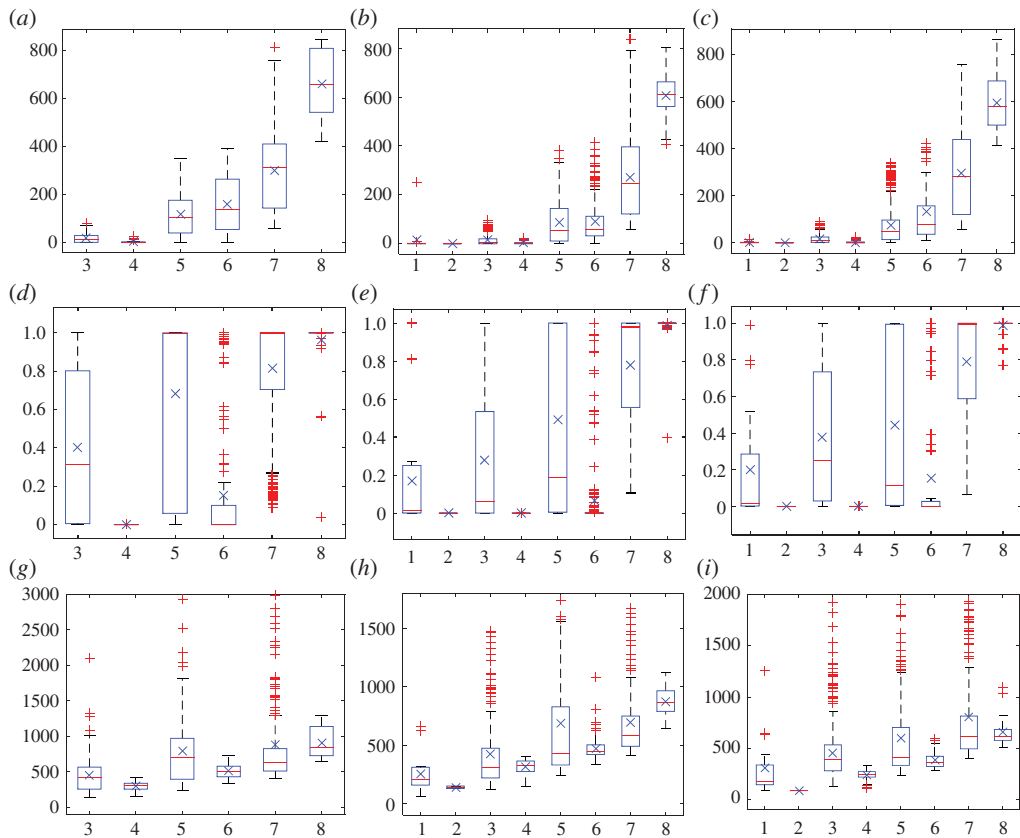


Figure 6. Box plots of the risk and maximum level of extreme smog for each category. The horizontal axis is the eight categories. 1–8 represent I-R, I-L, II-R, II-L, III-R, III-L, IV-R, IV-L, respectively. (a–c) Box plots of N_{mean} from 2014 to 2016, respectively; the vertical axis is the number of hours. (d–f) Box plots of p_{level} from 2014 to 2016, respectively; the vertical axis is the probability. (g–i) Box plots of x_{return} from 2014 to 2016, respectively; the vertical axis is $\text{PM}_{2.5}$ concentration ($\mu\text{g m}^{-3}$). In 2014, there are no stations in group I. In each box plot, points are drawn as outliers if they are larger than $q_3 + 1.5(q_3 - q_1)$ or smaller than $q_1 - 1.5(q_3 - q_1)$, where q_1 and q_3 are the 25th and 75th percentiles, respectively. The 1.5 corresponds to approximately $\pm 2.7\sigma$ and 99.3% coverage if the data are normally distributed. The plotted whiskers show the most extreme data values that are not outliers.

concern and anxiety it causes, the breaking probability for stations in categories IV-L and IV-R will be taken into account in this paper when proposing the goals for smog control.

In some circumstances, it is not very practical to set control goals using probability. Therefore, the 1-year return level (x_{return}) was computed using equation (2.6). x_{return} indicates the maximum value of extreme smog occurring on average once in every year. Figure 6g–i shows the box plot of x_{return} . Similar to the above case, due to the long tail density of extreme smog, the return levels for stations in categories II-R, III-R and IV-R showed extreme observations. The existence of extreme observations is precisely the reason for distinguishing between different categories to guarantee that very high extreme smog is targeted and treated specifically. For stations in category IV-L, the maximum values of extreme smog occurring on average once a year were very high. Their means or medians were $800 \mu\text{g m}^{-3}$ in 2014 and 2015, which dropped to $600 \mu\text{g m}^{-3}$ in 2016, which is still a very high level.

Beijing–Tianjin–Hebei will be used as an example to give specific results, because of the severity of extreme smog in this region, as well as its vital economic status in China, i.e. covering the capital and the most important port in northern China. It is worth noting that the breaking probability for stations in Beijing–Tianjin–Hebei was equal or very close to 1, implying that the

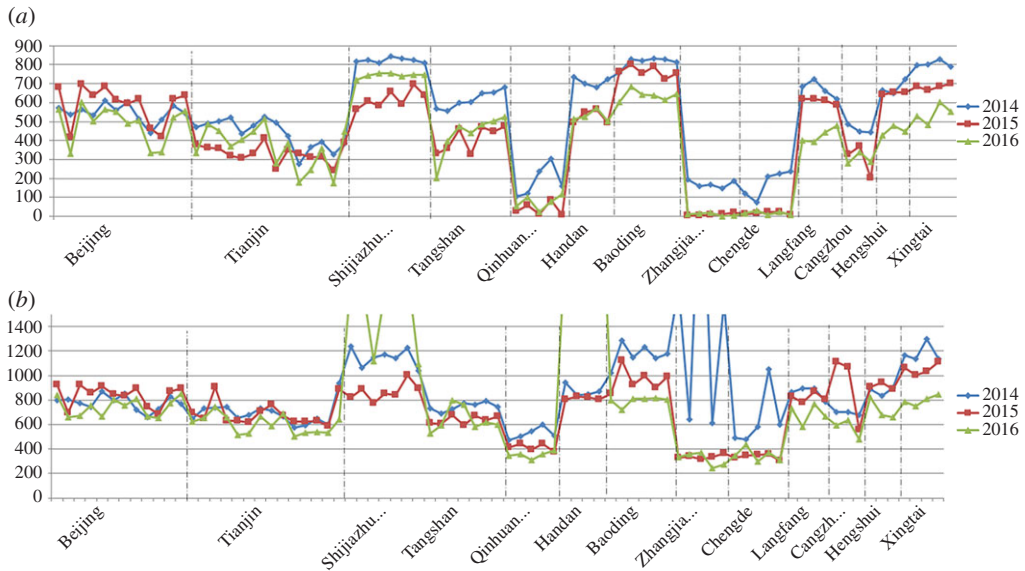


Figure 7. The risk and return level of extreme smog for the cities of Beijing–Tianjin–Hebei. (a) A line graph of N_{mean} from 2014 to 2016, respectively; the vertical axis is the number of hours. (b) A line graph of x_{return} from 2014 to 2016, respectively; the vertical axis is $\text{PM}_{2.5}$ concentration ($\mu\text{g m}^{-3}$). Note that values larger than $1400 \mu\text{g m}^{-3}$ are truncated here in order to display an overall visual impression.

occurrence of very high $\text{PM}_{2.5}$ concentrations in most of this area. The above three quantities, especially the hazardous hours (N_{mean} , figure 7a) and the 1-year return level (x_{return} , figure 7b), are further used to evaluate the performance of extreme smog control in Beijing–Tianjin–Hebei cities, which are summarized into the four cases mentioned below. Such an analysis, representing the worst case scenarios for certain individual high levels of extreme smog, also implied the results based on the feature of extreme smog.

The best performing cities were: Zhangjiakou, Chengde in the north of Hebei, and Qinhuangdao in the east of Hebei. The average hazardous hours within 1 year dropped dramatically to close to zero for stations in Zhangjiakou and Chengde during 2015; they were less than or equal to 100 h for stations in Qinhuangdao. The return levels for stations in the above cities declined as well, to about $300 \mu\text{g m}^{-3}$ in 2016. The performance of these cities on extreme smog control was superior to other cities in recent years, while the average levels of extreme smog in these cities also reduced.

Cities that barely improved or are getting worse: Beijing and Tianjin, Shijiazhuang (the provincial capital). N_{mean} and x_{return} for stations in Beijing and Tianjin hardly improved during 2014–2016, meaning the risk of extreme smog remained at a very high level. As discussed in the previous section on the features of extreme smog, stations in Beijing changed from category IV-L to category IV-R. The right skewness also implies the existence of an occasional very high level of extreme smog. Even worse, although similar category changes also happened in Shijiazhuang, the number of hazardous hours within 1 year increased in 2016 compared with 2015, which meant that this city was ranked the last among all cities of Beijing–Tianjin–Hebei. Moreover, the 1-year return level surged in 2016, indicating that the current treatment strategy is not very successful, especially on very high levels of $\text{PM}_{2.5}$.

Improved severely polluted cities: Baoding, Langfang in the middle of Hebei, Hengshui and Xingtai in the south of Hebei. There was a steady decline in N_{mean} and x_{return} during 2014–2016 (except for the return level of Hengshui in 2015), showing continuing effects of pollution abatement in these four cities. However, the original pollution levels of these cities were relatively high; in spite of the dramatic improvement, the current levels of extreme smog remained very high. This is also the reason why stations in these cities remained in category IV-L until 2016.

Ambiguous cities: the remaining three cities (Tangshan, Cangzhou and Handan). Stations in these cities did show some improvement in N_{mean} in 2015 but did not in 2016. There was no consensus as far as the improvement in the 1-year return level was concerned either. Therefore, the conclusions were ambiguous for these cities and the current measures were not qualified.

5. Discussion

By using the hourly PM_{2.5} data drawn from 945 stations across China, this study recognizes China's smog extremes by exploring systematic statistical analysis of the extreme smog in China and demonstrates its nationwide spatial patterns and characteristics. Stations across China are classified into eight categories according to the average level of extreme smog and the shape of the GEV density. Stations within different categories show different features of extreme smog. Under a similar average level of extreme smog, a station with a left-skewed density will have more values clustered at a high PM_{2.5} level so that the air quality is more often poor. Stations with right-skewed densities show occasional very high PM_{2.5} levels, significantly increasing their average levels, although the PM_{2.5} level at the maximum frequency is relatively low. The features of extreme smog discussed here, driven by the estimated mean and the shape parameter of the GEV distribution, provide more information than an average can, such as the maximum level of extreme smog with exact probabilities and the risk of experiencing certain levels of extreme smog. The analyses conducted in this study are better than other analyses applying a conventional mean analysis approach whose focus was on the average levels of smog, i.e. not on the extreme levels of smog which are mostly concerned by a pre-warning system.

We suggest that cities rather than stations are considered as the basic unit for smog prevention and control to facilitate governance by the authority. Specifically, cities belonging to different categories are advised to adopt different extreme smog prevention strategies. For cities belonging to categories I-L, II-L, III-L, IV-L, targeted measures should be used for all sources of pollutants, and normalized emission reductions should be implemented to alleviate the frequently occurring high PM_{2.5} concentrations. For cities belonging to the I-R, II-R, III-R, IV-R categories, it is more effective to target the related cause to lower the occasional very high PM_{2.5} values. Especially, cities within categories IV-R and IV-L should be considered as key areas that need to be focused on. More strict regulations regarding pollution emission, tax and fee collection, motor vehicle administration and coal burning control should be implemented, especially in those cities in the second and third cases in the last section. For the ambiguous cities, effective measures should be adhered to, and ineffective ones should be abandoned. Meanwhile, cities within the same category should jointly carry out severe atmosphere pollution forecasts, establish a pre-warning system for heavy pollution weather and develop a linked emergency response system.

The classification of stations in our work may provide a benchmark for air pollution joint prevention and control by the Chinese government and may be suitable as the basic unit for further analysis within each category. Cities within the same or similar category, especially those that are connected to each other, could be set as the basic unit to form one joint prevention and control region. Neighbouring cities could be incorporated to enlarge the joint region. Moreover, the level of extreme smog rather than the discharge capacity only should be taken into account when the emission reduction ratios are considered for cities in the joint region.

Extreme smog is much more hazardous to human health and welfare. The control goals proposed by this paper are aimed towards extreme smog reduction. It is again worth noting that the limits regarding PM_{2.5} concentration that must not be exceeded are almost certain to be violated in practice [51]. A more logical prevention goal for PM_{2.5} control would be regarding a maximum concentration with an acceptable return period or with an acceptable number of recurrence times during a certain time period. Therefore, the three quantities mentioned in the last section are more suitable for setting the control goals. Since the 1-year return levels for stations in Beijing–Tianjin–Hebei were very high, the short-term goals could be trying to decrease the 1-year return levels, or, in other words, to extend the return period of those levels to more than 1 year.

The long-term goals could be attempting to reduce the number of hazardous hours within 1 year or to extend the time interval of the hazardous smog's recurrence. Moreover, because the breaking probability was 1 for all the category IV-L stations and the attention this receives from the general public, the future goals could also be cutting down the breaking times. This is also useful for the establishment of a pre-warning and response system in that different levels of pre-warning could also be considered when a certain level of extreme smog is forecast to appear within a few days, or the breaking probability is very high, or the return level is predicted to approach certain limits.

Finally, extreme smog often occurred in several provinces of China during the same period, covering hundreds of square kilometres. For example, during February 2014, smog with long-term duration and high-level pollution blanketed 180 km² of China, including 15 provinces. Considering the close connections between stations within the same category, we can conclude that there must be some relationship between extreme smog at the stations within the categories. This kind of dependence, i.e. extreme dependence [52–54], should be explored in future studies so that the co-movement of extreme smog in different areas can be determined.

Data accessibility. The data source of PM_{2.5} is the China National Environmental Monitoring Centre (www.cnemc.cn).

Authors' contributions. Z.Z. and L.D. designed the project. L.D. performed the programming of observational data analyses and wrote the paper, with input from Z.Z. Both authors discussed the results and commented on the manuscript.

Competing Interests. We have no competing interests.

Funding. Funding for this research was provided by the National Natural Science Foundation of China (no. 71401189). The research was partially supported by the School of Statistics and Mathematics at the Central University of Finance and Economics.

References

1. Chen SM, He LY. 2014 Welfare loss of China's air pollution: how to make personal vehicle transportation policy. *China Econ. Rev.* **31**, 106–118. (doi:10.1016/j.chieco.2014.08.009)
2. Pearson JF, Goldfine AB, Bachireddy C, Brownstein JS, Shyamprasad S. 2010 Association between fine particulate matter and diabetes prevalence in the U.S. *Diabetes Care* **33**, 2196–2201. (doi:10.2337/dc10-0698)
3. Yang GH, Zhong NS. 2008 Effect on health from smoking and use of solid fuel in China. *Lancet* **372**, 1445–1446. (doi:10.1016/S0140-6736(08)61346-X)
4. Jonathan W. 2005 China: the air pollution capital of the world. *Lancet* **366**, 1671–1672.
5. Chen YY, Ebenstein A, Greenstone M, Lie HB. 2013 Evidence on the impact of sustained exposure to air pollution on life expectancy from China's Huai River policy. *Proc. Natl. Acad. Sci. USA* **110**, 12 936–12 941. (doi:10.1073/pnas.1300018110)
6. Huo H, Zhang Q, Guan DB, Su X, Zhao HY, He KB. 2014 Examining air pollution in China using production- and consumption-based emissions accounting approaches. *Environ. Sci. Technol.* **48**, 14 139–14 147. (doi:10.1021/es503959t)
7. Muller NZ, Mendelsohn R, Nordhaus W. 2011 Association environmental accounting for pollution in the United States economy. *Am. Econ. Rev.* **101**, 1649–1675. (doi:10.1257/aer.101.5.1649)
8. Lee JH. 2014 The sociological analysis on the smog of China: the perspective of complex risk society. *J. North-east Asian Cult.* **1**, 211–225. (doi:10.17949/jneac.1.41.201412.012)
9. Liu J, Gui H, Xie P, Liu W. 2015 Recent progress of atmospheric haze monitoring technology. *J. Atmos. Environ. Opt.* **10**, 93–101. (doi:10.3969/j.issn.1673-6141.2015.02.002)
10. Yuan Y, Liu S, Castro R, Pan X. 2012 PM_{2.5} monitoring and mitigation in the cities of China. *Environ. Sci. Technol.* **46**, 3627–3628. (doi:10.1021/es300984j)
11. Liu YS, Li YH, Chen C. 2015 Pollution: build on success in China. *Nature* **517**, 145–145. (doi:10.1038/517145d)
12. Qiu J. 2014 Fight against smog ramps up. *Nature* **506**, 273–274. (doi:10.1038/506273a)
13. Li X, Lin C, Wang Y, Zhao LY, Duan N, Wu XD. 2015 Analysis of rural household energy consumption and renewable energy systems in Zhangziying town of Beijing. *Ecol. Model.* **318**, 184–193. (doi:10.1016/j.ecolmodel.2015.05.011)

14. Shi H, Wang Y, Huisingh D, Wang J. 2014 On moving towards an ecologically sound society: with special focus on preventing future smog crises in China and globally. *J. Clean. Prod.* **64**, 9–12. (doi:10.1016/j.jclepro.2013.07.024)
15. Chang Y. 2012 China needs a tighter PM_{2.5} limit and a change in priorities. *Environ. Sci. Technol.* **46**, 7069–7070. (doi:10.1021/es3022705)
16. Zhang JF, Samet JM. 2015 Chinese haze versus Western smog: lessons learned. *J. Thorac. Dis.* **7**, 3–13. (doi:10.3978/j.issn.2072-1439.2014.12.06)
17. Ouyang YD. 2014 Features: China seeks creative ways to combat smog. *Lancet Respir. Med.* **2**, 794–794. (doi:10.1016/S2213-2600(14)70138-9)
18. Zhang DY, Liu JJ, Li BJ. 2014 Tackling air pollution in China—what do we learn from the great smog of 1950s in London. *Sustainability* **6**, 5322–5338. (doi:10.3390/su6085322)
19. Wang L. 2014 The battle against PM_{2.5} is on. *Natl. Sci. Rev.* **1**, 315–317. (doi:10.1093/nsr/nwu016)
20. Xu H, Bi XH, Zheng WW, Wu JH, Feng YC. 2015 Particulate matter mass and chemical component concentrations over four Chinese cities along the western Pacific coast. *Environ. Sci. Pollut. R* **22**, 1940–1953. (doi:10.1007/s11356-014-3630-0)
21. Chang SY, Chou CC, Liu S, Zhang Y. 2013 The characteristics of PM_{2.5} and its chemical compositions between different prevailing wind patterns in Guangzhou. *Aerosol. Air Qual. Res.* **13**, 1373–1383. (doi:10.4209/aaqr.2012.09.0253)
22. Li J *et al.* 2014 Chemical characteristics and source apportionment of PM_{2.5} during the harvest season in eastern China's agricultural regions. *Atmos. Environ.* **92**, 442–448. (doi:10.1016/j.atmosenv.2014.04.058)
23. Yang F *et al.* 2011 Characteristics of PM_{2.5} speciation in representative megacities and across China. *Atmos. Chem. Phys.* **11**, 5207–5219. (doi:10.5194/acp-11-5207-2011)
24. Huang RJ *et al.* 2014 High secondary aerosol contribution to particulate pollution during haze events in China. *Nature* **514**, 218–222. (doi:10.1038/nature13774)
25. Zhang R *et al.* 2015 Formation of urban fine particulate matter. *Chem. Rev.* **115**, 3803–3855. (doi:10.1021/acs.chemrev.5b00067)
26. Wang XM, Chen JM, Cheng TT, Zhang RY, Wang XM. 2014 Particle number concentration, size distribution and chemical composition during haze and photochemical smog episodes in Shanghai. *J. Environ. Sci. (China)* **26**, 1894–1902. (doi:10.1016/j.jes.2014.07.003)
27. Liu JW *et al.* 2014 Source apportionment using radiocarbon and organic tracers for PM_{2.5} carbonaceous aerosols in Guangzhou, south China: contrasting local- and regional-scale haze events. *Environ. Sci. Technol.* **48**, 12 002–12 011. (doi:10.1021/es503102w)
28. Cao C *et al.* 2014 Inhalable microorganisms in Beijing's PM_{2.5} and PM₁₀ pollutants during a severe smog event. *Environ. Sci. Technol.* **48**, 1499–1507. (doi:10.1021/es4048472)
29. Guo S *et al.* 2014 Elucidating severe urban haze formation in China. *Proc. Natl. Acad. Sci. USA* **111**, 17 373–17 378. (doi:10.1073/pnas.1419604111)
30. Huang K *et al.* 2014 Extreme haze pollution in Beijing during January 2013: chemical characteristics, formation mechanism and role of fog processing. *Atmos. Chem. Phys. Discuss.* **14**, 7517–7556. (doi:10.5194/acpd-14-7517-2014)
31. He H *et al.* 2015 Analysis of the causes of heavy aerosol pollution in Beijing, China: a case study with the WRF-Chem model. *Particuology* **20**, 32–40. (doi:10.1016/j.partic.2014.06.004)
32. Uno I, Sugimoto N, Shimizu A, Yumimoto K, Hara Y, Wang Z. 2014 Record heavy PM_{2.5} air pollution over China in January 2013: vertical and horizontal dimensions. *SOLA* **10**, 136–140. (doi:10.2151/sola.2014-028)
33. Wang L, Zhang N, Liu Z, Sun Y, Ji D, Wang Y. 2014 The influence of climate factors, meteorological conditions, and boundary-layer structure on severe haze pollution in the Beijing-Tianjin-Hebei region during January 2013. *Adv. Meteorol.* **2014**, 685971. (doi:10.1155/2014/685971)
34. Sun Y *et al.* 2014 Investigation of the sources and evolution processes of severe haze pollution in Beijing in January 2013. *J. Geophys. Res.* **119**, 4380–4398. (doi:10.1002/2014JD021641)
35. Qi Y, Fang SB, Zhou WZ. 2015 Correlative analysis between the changes of surface solar radiation and its relationship with air pollution, as well as meteorological factor in East and West China in recent 50 years. *Acta Phys. Sin.* **64**, 089201. (doi:10.7498/aps.64.089201)
36. Chen J *et al.* 2014 Impact of relative humidity and water soluble constituents of PM_{2.5} on visibility impairment in Beijing, China. *Aerosol. Air Qual. Res.* **14**, 260–268. (doi:10.4209/aaqr.2012.12.0360)

37. Zhao HY *et al.* 2015 Assessment of China's virtual air pollution transport embodied in trade by using a consumption-based emission inventory. *Atmos. Chem. Phys.* **15**, 5443–5456. (doi:10.5194/acp-15-5443-2015)
38. Liang X *et al.* 2015 Assessing Beijing's PM_{2.5} pollution: severity, weather impact, APEC and winter heating. *Proc. R. Soc. A* **471**, 20150257. (doi:10.1098/rspa.2015.0257)
39. Lin G *et al.* 2014 Spatio-temporal variation of PM_{2.5} concentrations and their relationship with geographic and socioeconomic factors in China. *Int. J. Environ. Res. Public Health* **11**, 173–186. (doi:10.3390/ijerph110100173)
40. van Donkelaar A *et al.* 2010 Global estimates of ambient fine particulate matter concentrations from satellite-based aerosol optical depth: development and application. *Environ. Health Persp.* **118**, 847–855. (doi:10.1289/ehp.0901623)
41. van Donkelaar A *et al.* 2015 Use of satellite observations for long-term exposure assessment of global concentrations of fine particulate matter. *Environ. Health Persp.* **123**, 135–143. (doi:10.1289/ehp.1408646)
42. U.S. EPA. 2012 Fact Sheet: Revised air quality standards for particle pollution and updates to the air quality index (AQI). See <http://www.epa.gov/airquality/particlepollution/2012/decfsstandards.pdf> (accessed 25Apr 2016).
43. Coles S. 2001 *An introduction to statistical modeling of extreme values*. Berlin, Germany: Springer.
44. Smith RL. 2003 Statistics of extremes, with applications in the environment, insurance and finance. In *Extreme value in finance, telecommunications and the environment* (eds B Finkenstadt, H Rootzen). Boca Raton, FL: Chapman and Hall/CRC.
45. Benjamini Y, Hochberg Y. 1995 Controlling the false discovery rate: a practical and powerful approach to multiple testing. *J. R. Stat. Soc. B* **57**, 289–300.
46. Benjamini Y, Yekutieli D. 2001 The control of the false discovery rate in multiple testing under dependency. *Ann. Stat.* **29**, 1165–1188.
47. Luo Y, Lu D, Zhou X, Li W, He Q. 2001 Characteristics of the spatial distribution and yearly variation of aerosol optical depth over China in last 30 years. *J. Geophys. Res.* **106**, 14 501–14 513. (doi:10.1029/2001jd900030)
48. Xu L, Liu L, Zhang J, Zhang Y, Ren Y, Wang X, Li W. 2017 Morphology, composition, and mixing state of individual aerosol particles in Northeast China during wintertime. *Atmosphere* **8**, 2017. (doi:10.3390/atmos8030047)
49. Ministry of Environmental Protection of the People's Republic of China. 2016 China environmental status bulletin 2015. *Environmental Protection* **11**, 43–51.
50. Ministry of Environmental Protection of the People's Republic of China. China environmental status bulletin 2016. See <http://www.mep.gov.cn/gkml/hbb/qt/201706/W020170605812243090317.pdf>.
51. Roberts EM. 1979 Review of statistics of extreme values with applications to air quality data. Part I. Review. *J. Air Pollut. Control Assoc.* **29**, 632–637. (doi:10.1080/00022470.1979.10470835)
52. Sibuya M. 1960 Bivariate extreme statistics, I. *Ann. Inst. Statist. Math* **11**, 195–210. (doi:10.1007/BF01682329)
53. Zhang Z. 2008 Quotient correlation: a sample-based alternative to Pearson's correlation. *Ann. Stat.* **36**, 1007–1030. (doi:10.1214/009053607000000866)
54. Zhang Z, Zhang C, Cui Q. 2017 Random threshold driven tail dependence measures with application to precipitation data analysis. *Stat. Sin.* **27**, 685–709.